Wave packet simulations for the insulator–metal transition in dense hydrogen

2009 J. Phys. A: Math. Theor. 42 214055

(http://iopscience.iop.org/1751-8121/42/21/214055)

IOP PUBLISHING JOURNAL OF PHYSICS A: MATHEMATICAL AND THEORETICAL

J. Phys. A: Math. Theor. **42** (2009) 214055 (9pp) doi:10.1088/1751-8113/42/21/214055

Wave packet simulations for the insulator–metal transition in dense hydrogen

B Jakob, P-G Reinhard, C Toepffer and G Zwicknagel

Institut für Theoretische Physik II, Universität Erlangen, Staudtstr. 7, D-91058 Erlangen, Germany

Received 28 August 2008, in final form 19 November 2008
Published 8 May 2009
Online at stacks.iop.org/JPhysA/42/214055

Abstract

Dense hydrogen is studied in the framework of wave packet simulations. In this semi-quantal method the electrons are represented by wave packets which are suitably parameterized, e.g. Gaussians. The time evolution of the system and the equilibrium properties are obtained with the help of a variational principle and by Monte Carlo sampling, respectively. A transition from a molecular to a metallic state is observed. The wave packets become delocalized and the electrical conductivity increases sharply. The phase diagram is calculated in a wide range of the pressure–density–temperature space. In the transition from the molecular to the metallic state the density increases in agreement with recent reverberating shock wave experiments.

PACS numbers: 52.65.Yy, 02.70.Ns, 05.70.Ce, 62.50.+p

1. Introduction

Although hydrogen is the simplest of all chemical elements and the Coulomb interaction between the constituents has been known for more than two centuries, its physical properties under extreme conditions still constitute a great challenge to many-body physics. A transition to a metallic phase has been predicted by extrapolation of experimental results [1]. Complementary shock wave experiments show direct evidence for such a transition [2, 3]. However, the strong compression observed in earlier measurements with the Nova Laser [4] has not been confirmed in more recent experiments with the *Z* machine [5] or with explosives [6]. The equation of state of hydrogen determines the structure of brown dwarfs and giant gas planets [7, 8]. It must also be known for the production of energy by inertial fusion of deuterium pellets [9].

The possibility of a metalization of hydrogen at high densities was discussed already in 1935 by Wigner and Huntington [10]. Since then a large number of theoretical methods have been employed in this connection. On one hand, there is the chemical picture [11] where the free energy of a system consisting of components, such as H_2, H, protons, electrons, . . . ,

is minimized [7, 12]. This requires effective interactions, pair correlations, exchange parts and polarization corrections as input [13]. In contrast the 'ab initio' methods start on a more fundamental level, but for practical solutions approximations must be made. Usually the attention is focused on the electrons while the nuclei are supposed to move classically because of their large mass. In tight-binding molecular dynamics (TBMD) the forces on the nuclei are obtained from the total energy of bound electrons whose wavefunctions are parameterized to fit the H_2-molecule and other suitable data [14]. Alternatively the electron energy is calculated in the local density approximation (LDA) of the density functional theory (DFT) [15, 16]. In recent work the generalized gradient approximation (GGA) is used for the exchange and correlation energies, see, e.g. [17–19]. These are low-temperature methods as long as the underlying density functionals are independent of the temperature. The density can also be calculated by a Monte Carlo evaluation of path integrals (PIMC). Because of the fermion sign problem the paths are restricted in order to avoid the crossing of nodes of the free system [20]. So this RPIMC is rather a high-temperature method [21]. More recent reformulations aim at a representation of the exchange problem in the form of a Slater determinant [22]. To close the methodical gap at intermediate temperatures, coupled electronic–ionic Monte Carlo (CEIMC) calculations have been made [23]. These use the Born–Oppenheimer approximation and require a careful choice of trial functions. Some currently most favored implementations of density functional and quantum Monte Carlo many-body methods have been presented on this conference, see, e.g., [24, 25].

Here we present results from wave packet (WP) simulations for the metalization of hydrogen. In this method [26, 27], the electron wavefunctions are represented by moving Gaussians of variable width. In earlier application to dense matter various compromises were made in respect to the fermion problem which limited the regime of application [28, 29]. In the present calculations, the anti-symmetrization is fully implemented [30, 31]. This prevents an unphysical growth of the overlap of the wave packets and thus the growth of their widths. There is no more need for introducing an ad hoc potential to limit the spread of the wave packets. The focus of the present paper lies on results which have not been published previously. While the method is briefly described in section 2 we discuss in section 3 some new results for the metalization of hydrogen. Our conclusions are presented in section 4.

2. Wave packet simulations

A cubic simulation box of length L containing N electrons and protons is periodically continued to represent the bulk system. The protons are treated classically because of their large mass. The electrons are described by the fully anti-symmetrized product

$$\Psi_{\vec{q}}(\vec{x}_1, \ldots, \vec{x}_N, t) = \frac{1}{\sqrt{N}} \sum_{\sigma \in P} \mathrm{sgn}(\sigma) \prod_{k=1}^{N} \varphi_{k,\vec{q}_k}(\vec{x}_{\sigma_k}) \tag{1}$$

of the single-particle Gaussian wavefunctions

$$\varphi_{k,\vec{q}}(\vec{x}, t) = \mathrm{e}^{\mathrm{i}\vec{q}\cdot\vec{x}} \sum_{\vec{n}\in\mathbb{Z}^3} \exp\left[-\left(\frac{3}{4\gamma_k^2} - \frac{\mathrm{i}p_{\gamma_k}}{2\gamma_k} \right) (\vec{x}_k - \vec{r}_k - \vec{n}L)^2 + \mathrm{i}\vec{p}_k \cdot (\vec{x} - \vec{r}_k - \vec{n}L) \right] \tag{2}$$

depending on the Bloch-momentum $\vec{q}$ and the parameters $\{v_k(t)\} = \{\vec{r}_k(t), \gamma_k(t), \vec{p}_k(t), p_{\gamma_k}(t)\}$ representing the position and the width of the Gaussian $\vec{r}_k(t)$, $\gamma_k(t)$, respectively, and their conjugate momenta $\vec{p}_k(t)$, $p_{\gamma_k}(t)$. As these basis states are not orthonormal

$$\langle \varphi_{k,\vec{q}} | \varphi_{l,\vec{q}'} \rangle = (O)_{kl} \delta^3(\vec{q} - \vec{q}'), \tag{3}$$

a (formal) orthonormalization

$$|\tilde{\varphi}\rangle = Y^{1/2}|\varphi\rangle \tag{4}$$

with $Y = O^{-1}$ allows the evaluation of all anti-symmetrized matrix elements of the hydrogen Hamiltonian

$$\hat{H} = \hat{T}_{\text{ion}} + \hat{t}_{\text{el}} + \hat{V}_{\text{ion-ion}} + \hat{V}_{\text{ion-el}} + \hat{V}_{\text{el-el}} \tag{5}$$

with Coulomb interactions $\hat{V}$ in Fourier space by numerically robust $O(N^3)$ matrix operations. For example, for the electron kinetic energy

$$E_{\text{kin}} = \sum_{k=1}^{N} \int \mathrm{d}^3 g \, \langle \tilde{\varphi}_{k,\vec{q}} | \hat{t} | \tilde{\varphi}_{k,\vec{q}} \rangle = \mathrm{Tr}\,(\mathbf{t} \cdot \mathbf{Y}) + E_{\text{Bloch}}. \tag{6}$$

Here, E_{Bloch} is a grid energy which depends on the ratio of the width γ to the box size L [31].

2.1. Wave packet molecular dynamics (WPMD)

For the dynamics of the system, the time evolution of the parameters $v_k(t)$ is obtained from the time-dependent variational principle minimizing the action $\int \mathcal{L}[\Psi, \Psi^*]\,\mathrm{d}t$ with the Lagrangian

$$\mathcal{L}[\Psi, \Psi^*] = \langle \Psi(t) | \mathrm{i}\hbar \frac{\partial}{\partial t} - \hat{H} | \Psi(t) \rangle. \tag{7}$$

With the expectation value $\mathcal{H}\{v\} = \langle \Psi | \hat{H} | \Psi \rangle$ and the norm matrix $\mathcal{N}$ with elements

$$(\mathcal{N})_{ij} = -2\hbar\, \mathrm{Im} \left\langle \frac{\partial}{\partial v_i} \Psi \middle| \frac{\partial}{\partial v_j} \Psi \right\rangle \tag{8}$$

there result non-symplectic equations of motion for the parameters

$$\dot{v}_i = \sum_{j=1}^{n} (\mathcal{N}^{-1})_{ij} \frac{\partial \mathcal{H}}{\partial v_j}. \tag{9}$$

Here the propagation of the wave packets is treated in real time in some analogy to variational calculations of the density at finite temperatures [32]. The variational density matrix (VDM) serves as a suitable input to RPIMC calculations [21].

2.2. Wave packet Monte Carlo simulations

The equilibrium properties at a certain temperature $T = (\beta k_{\text{B}})^{-1}$ can be obtained by Monte Carlo sampling. For that purpose one conceives a transformation to canonical coordinates $\{v\} \to \{u\}$

$$\mathrm{d}\vec{u} = \mathcal{B}\, \mathrm{d}\vec{v} \tag{10}$$

with

$$\mathcal{B}\mathcal{N}^{-1}\mathcal{B} = \begin{pmatrix} 0 & \mathbb{1} \\ -\mathbb{1} & 0 \end{pmatrix} \tag{11}$$

for which the equations of motion are symplectic. In these coordinates the expectation value of a dynamical variable A is

$$\bar{A} = \frac{1}{Z} \int \mathrm{d}^M u \, \mathrm{e}^{-\beta \mathcal{H}\{u\}} A\{u\} \tag{12}$$

with $Z = \int \mathrm{d}^M u \, \mathrm{e}^{-\beta \mathcal{H}\{u\}}$. As $\mathrm{d}^M u = |\det \mathcal{B}|\, \mathrm{d}^M v = (\det \mathcal{N})^{\frac{1}{2}}\, \mathrm{d}^M v$

$$\bar{A} = \frac{1}{Z} \int \mathrm{d}^M v \, (\det \mathcal{N})^{\frac{1}{2}} \, \mathrm{e}^{-\beta \mathcal{H}\{v\}} \, A\{v\} \tag{13}$$

with $Z = \int \mathrm{d}^M v (\det \mathcal{N})^{\frac{1}{2}} \mathrm{e}^{-\beta \mathcal{H}\{v\}}$. This serves as a starting point for the calculation of equilibrium properties by wave packet Monte Carlo simulations [30]. Without anti-symmetrization the modified volume element in expression (13) would be equal to 1. As the overlap of the wave packets increases with their width the presence of the modified volume element prevents an unphysical growth of the widths of the wave packets.

2.3. Virial theorem

The key observable in most measurements is the pressure P. In a Coulomb system of volume V, it can be expressed with the help of the virial theorem

$$P = \frac{1}{3}\left(2\frac{\bar{E}_{\mathrm{kin}}}{V} + \frac{\bar{E}_{\mathrm{pot}}}{V}\right) \tag{14}$$

through the expectation values of the kinetic and potential energies of the particles [33]. While being formally simple, this expression depends crucially on a subtle balance between kinetic and potential energy. For a test of the WP method, a comparison with the exactly known Hartree–Fock solution for the free electron gas and a simple one-component plasma (OCP) model for metallic hydrogen has been made [30, 31].

3. Metalization of hydrogen

3.1. Isothermal changes

The diamond anvil experiments for the isotherms of hydrogen and deuterium at room temperature [1] show hardly any difference between both isotopes, our simulations (typically $N = 250$) are therefore done for hydrogen only. The measurements up to a density $N/V = n = 0.72 \times 10^{30}$ m^{-3} show a smooth behavior of $P(n)$, with no indications of a phase transition. Here earlier results of our WP simulations [30, 31] show that the slope of $P(n)$ levels off near $n = 0.9 \times 10^{30}$ m^{-3}. At this density the average width of the wave packets jumps rather suddenly, the electrons delocalize and the system becomes conducting. The electrical conductivity is calculated with the help of WPMD simulations from the current–current autocorrelation function

$$\sigma = \frac{\beta}{3L^3}\int_0^{\tau\to\infty} \mathrm{d}t\, \overline{\vec{j}(t)\cdot\vec{j}(0)}. \tag{15}$$

At the critical density the conductivity jumps by some orders of magnitude. The transition to metallic state can also be visualized in terms of the spatial distribution of the particles. An inspection of the simulation box at $n = 0.2 \times 10^{30}$ m^{-3} shows a molecular sc crystal (a cubic structure is favored by the shape of the simulation box) with the electrons localized between the two protons of an H_2 molecule. Around $n = 0.6 \times 10^{30}$ m^{-3} the crystal begins to dissolve forming a molecular fluid. At $n = 0.9 \times 10^{30}$ m^{-3} the protons form a cubic bcc lattice with electrons moving freely between the sites. These qualitative pictures are supported by calculations of the pair distribution functions. At $n = 0.2 \times 10^{30}$ m^{-3} there is a strong nearest-neighbor peak at the bond length 0.8×10^{-10} m of the protons in the free H_2 molecule. The long-range order is washed out because of thermal vibration and molecular rotation. In the denser fluid regime these structures disappear until they re-emerge at higher densities $n = 0.9 \times 10^{30}$ m^{-3}, indicating the long-range metallic order. The electron-pair distribution has a peak near 0.4×10^{-10} m at $n = 0.2 \times 10^{30}$ m^{-3}, i.e. the electrons are concentrated between the two protons of the H_2 molecule. With increasing density this distribution function becomes flat. There is no enhancement near zero distance, which indicates that there are no atoms.

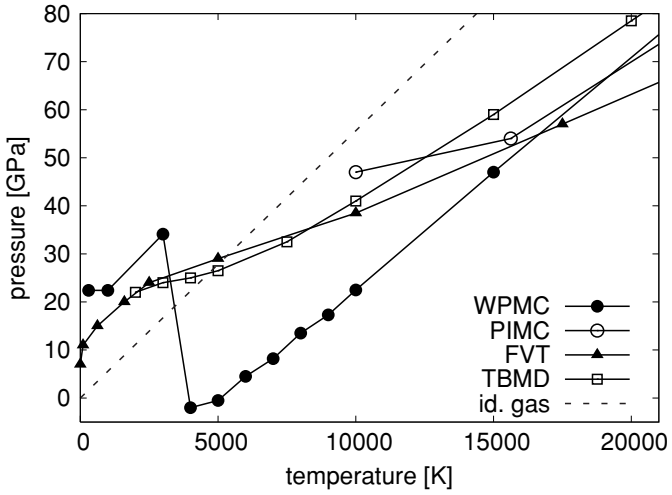

Figure 1. The hydrogen isochore $P(T)$ at $n = 0.2 \times 10^{30}$ m^{-3}: compared are results from WPMC simulations (filled circles), PIMC simulations [21] (open circles), fluid variational theory [34] (FVT, triangles), TBMD simulations [14] (open squares) and the ideal gas isochore (dashed-dotted).

3.2. Isochoric changes

In figure 1 we show an isochore $P(T)$ at $n = 0.2 \times 10^{30}$ m^{-3}. While the results from PIMC [21], fluid variational theory (FVT) [34] and TBMD [14] are rather featureless, the WPMC simulations show a sudden drop in pressure near 4000 K which is associated with an increase of the width of the wave packets. A similar feature has been observed in earlier PIMC simulations near 10 000 K [20].

Because of the Maxwell relation $(\partial P/\partial T)_V = (\partial S/\partial V)_T$ we expect that this decrease in the isochoric pressure corresponds at a constant temperature to an increase of the entropy with density, i.e. a transition to a less-ordered, denser metallic state. The negative pressure at $T = 4000$ K indicates an instability. There should be a phase separation with metallic drops immersed in a molecular fluid. Obviously such an inhomogeneous system cannot be properly described in the present simulations. At temperatures of $T = 3000$–4000 K, the proton–proton pair distribution function shows a moderately coupled proton OCP. At $T = 3000$ K, the electron–proton pair distribution is moderately enhanced near zero indicating the presence of a small fraction of atoms or atom-like structures during the change from the molecular regime at $T = 300$ K to the practical free-electron gas at $T = 4000$ K.

3.3. Phase diagram

The equilibrium properties of dense hydrogen were calculated by WPMC simulations in a broad range of parameters where a plasma phase transition, i.e. a first-order transition from a molecular to a metallic state, has been predicted, see, e.g. [8]. In the density range $n = (0.1$–$0.9) \times 10^{30}$ m^{-3} and temperatures up to $T = 4000$ K emerges a clear separation of a molecular phase (low T and low P) and a metallic phase [30, 31]. At the border between both regimes both phases coexist, the metallic phase being denser as the molecular one, as discussed above. Isolated points of the phase boundary curve have also been obtained by other methods [15–17], see, e.g. figure 9 of [31]. In figure 2 we show isotherms in the $n - P$ plane

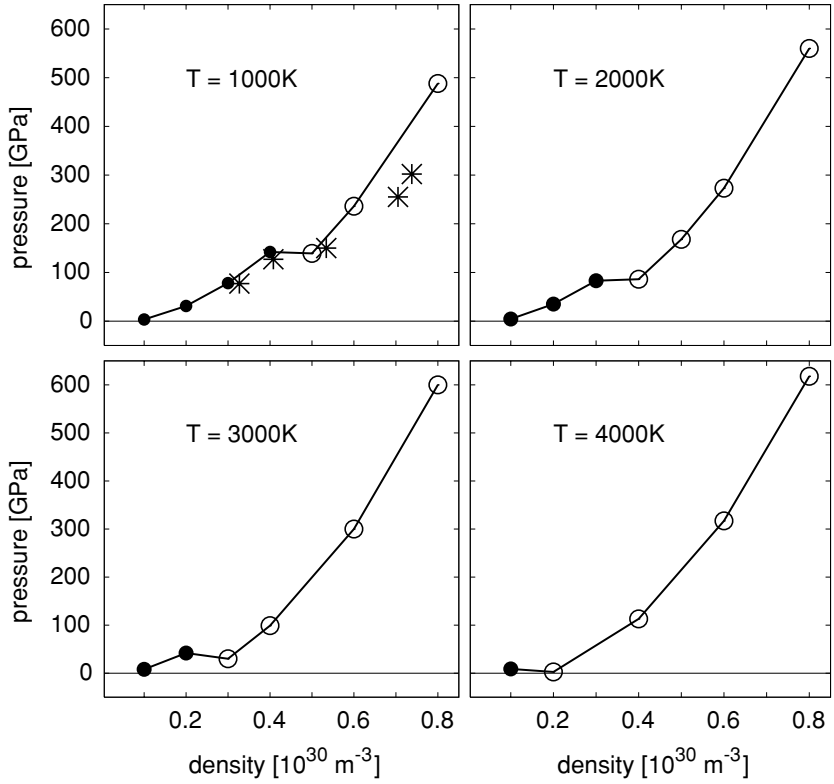

Figure 2. Hydrogen isotherm $P(n)$ obtained by WPMC simulations at $T = 1000$ K, 2000 K, 3000 K and 4000 K. Dots correspond to a molecular system, open circles to the metallic state. The stars indicate experimental results from a quasi-isentropic compression in this range of densities, temperatures and pressures [3].

which demonstrate a first-order transition from a molecular to a metallic state. Experimental evidence for such a transition in this range of densities, temperatures and pressures has recently been obtained by a quasi-isentropic compression of a deuterium plasma in reverberating shock wave experiments [3]. We included these measured data in the plot of our $T = 1000$ K isotherm. The coexistence region deduced from our simulations resembles very much the banana-like domain of a first-order insulator–metal transition [35] shown in figure 3.

3.4. Hugoniots

Unfortunately static experiments are increasingly difficult at high temperatures and pressures even for deuterium because diffusion limits the strength of the anvils. In shock wave experiments [4–6] there arose controversies in regard to the interpretation of the measurements: are the shock fronts planar, has an equilibrium been reached, etc? The conservation of mass, momentum and energy yields the Hugoniot relation for the change in internal energy, pressure and density across a shock front. The (desired) equation of state translates this into a density compression and an increase in pressure and temperature.

In figure 4 (left panel) we show the pressure as a function of the density compression for deuterium. The wave packet results [30] agree quite well with those of the FVT [36] and the linear mixing model [37] both at low and at high pressures, but the compression is even

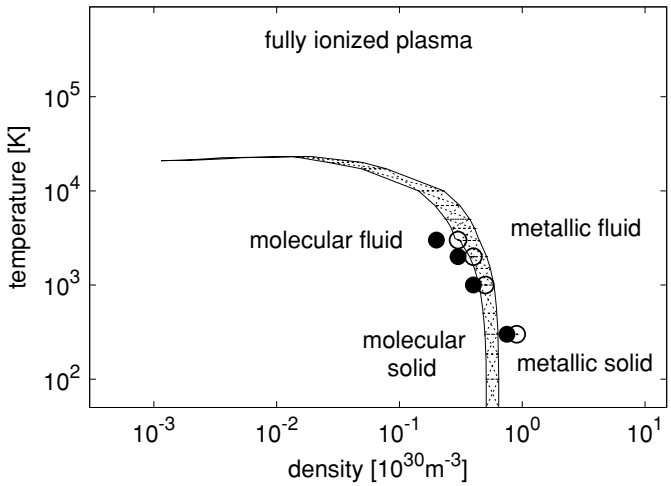

Figure 3. Coexistence region from the present WPMC simulations (filled circles for the molecular and open circles for the metallic boundary) compared with the coexistence region predicted in [35].

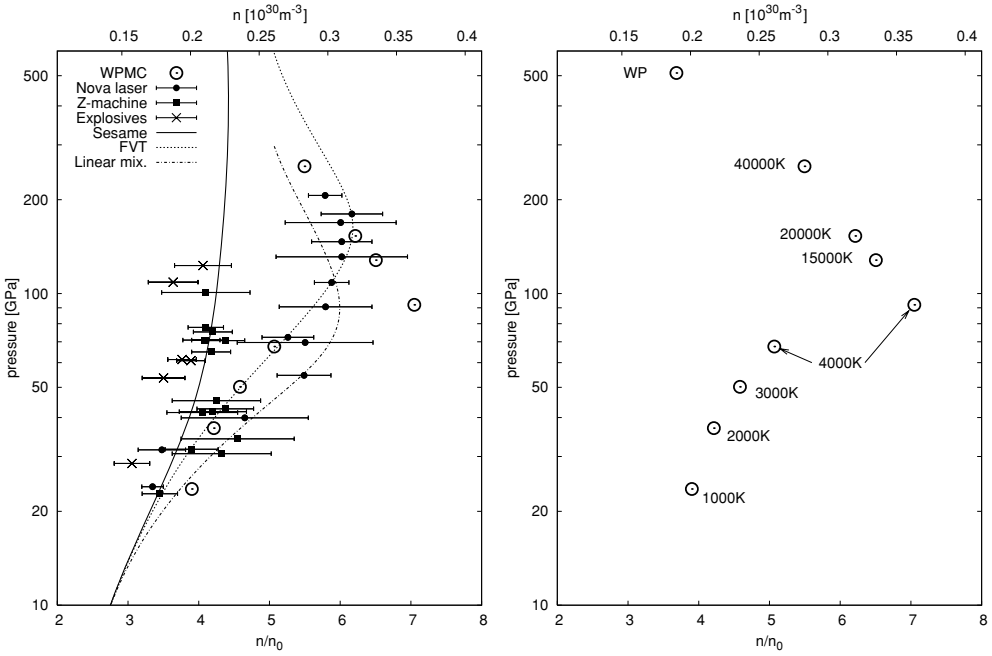

Figure 4. $P(n)$ under Hugoniot conditions. (Left panel) full curve: Sesame [38]; dashed-dotted curve: linear mixing [37]; dotted curve: FVT [36]; full squares: *Z* machine [5]; dots: Nova Laser [4]; crosses: explosives [6]; open circles: WPMC [30]. (Right panel) temperatures calculated in WPMC [30].

larger than in the NOVA experiments [4] in the intermediate range around 100 GPa. These became doubtful as more recent experiments at the *Z* machine [5] and with high explosiives [6] show a more modest compression which agrees with the Sesame table [38]. In the right

panel of figure 4 we show the temperatures reached along the Hugoniot according to the wave packet simulations. The disagreement with the data [5] and other subsequent calculations, e.g. [7, 18, 19], raises the question whether the present parameterization of the wave packets by the Gaussians given in equation (2) may be too rigid for a proper exploration of the many-body Hilbert space. The ground-state properties of simple systems such as H, H_2 and He have been discussed in [30]. In many-body systems at temperatures above 5000 K nodes in the trial function may be required. Rather than generalizing the trial functions one may attempt to modify the interactions. We note in this connection that a satisfactory agreement with the experiments [5, 6] is obtained by simplified wave packet simulations, where the explicit anti-symmetrization is replaced by a Pauli exclusion energy depending on the overlap of the wave packets and three parameters which were chosen to optimize small molecules like CH_4 [39].

4. Summary

In our fully anti-symmetrized wave packet simulations we have shown a first-order phase transition from molecular hydrogen to a metallic state. The following observables were investigated: isotherms $P(n)$, isochores $P(T)$, pair distribution functions and electrical conductivities. The metallic phase has a higher density than the molecular phase. Further work on the compressibility under Hugoniot conditions is desirable.

Acknowledgments

This work was supported by the Bundesministerium für Bildung und Forschung (06 ER 145) and by the Gesellschaft für Schwerionenforschung (GSI-ER/TOE).

References

[1] Loubeyre P, Occelli F and LeToullec R 2002 *Nature* **416** 613
[2] Nellis W J, Weir S T and Mitchell A C 1999 *Phys. Rev.* B **59** 3434
[3] Fortov V E *et al* 2007 *Phys. Rev. Lett.* **99** 185001
[4] Collins G W *et al* 1998 *Phys. Plasmas* **5** 1864
[5] Knudson M D, Hanson D L, Bailey J E, Hall C A, Asay J R and Deeney C 2004 *Phys. Rev.* B **69** 144209
[6] Boriskov G V, Bykov A I, Ilkaev R I, Selemir V D, Simakov G V, Trunin R F, Urlin V D, Shuikin A N and Nellis W J 2005 *Phys. Rev.* B **71** 092104
[7] Chabrier G, Saumon D, Hubbard W B and Lunine J I 1992 *Astrophys. J.* **391** 827
[8] Chabrier G, Saumon D and Potekhin A Y 2006 *J. Phys. A: Math. Gen.* **39** 4411
[9] Bennett G R *et al* 2002 *Phys. Rev. Lett.* **89** 245002
[10] Wigner E and Huntington H B 1935 *J. Chem. Phys.* **3** 764
[11] Kraeft W D, Kremp D, Ebeling W and Röpke G 1986 *Quantum Statistics of Charged Particle Systems* (Berlin: Akademie)
[12] Saumon D and Chabrier G 1992 *Phys. Rev.* A **46** 2084
[13] Juranek H, Redmer R and Rosenfeld Y 2002 *J. Chem. Phys.* **117** 1768
[14] Lenosky T J, Kress J D, Collins L A, Redmer R and Juranek H 1999 *Phys. Rev.* E **60** 1665
[15] Johnson K A and Ashcroft N W 2000 *Nature* **403** 632
[16] Scandolo S 2003 *Proc. Natl Acad. Sci. USA* **100** 3051
[17] Bonev S A, Schwegler E, Ogitsu T and Galli G 2004 *Nature* **431** 669
[18] Desjarlais M P 2003 *Phys. Rev.* B **68** 064204
[19] Holst B, Redmer R and Desjarlais M P 2008 *Phys. Rev.* B **77** 184201
[20] Magro W R, Ceperley D M, Pierleoni C and Bernu B 1996 *Phys. Rev. Lett.* **76** 1240
[21] Militzer B and Ceperley D M 2000 *Phys. Rev. Lett.* **85** 1890
[22] Bezkrovniy V, Filinov V S, Kremp D, Bonitz M, Schlanges M, Kraeft W D, Levashov P R and Fortov V E 2004 *Phys. Rev.* E **70** 057401

[23] Pierleoni C, Ceperley D M and Holzmann M 2004 *Phys. Rev. Lett.* **93** 146402
[24] Pierleoni C 2008 Talk given at this conference
[25] Militzer B 2009 *J. Phys. A: Math. Theor.* **42** 214001
[26] Heller E J 1975 *J. Chem. Phys.* **62** 1544
[27] Feldmeier H and Schnack J 2000 *Rev. Mod. Phys.* **72** 655
[28] Klakow D, Toepffer C and Reinhard P-G 1994 *J. Chem. Phys.* **101** 10766
[29] Knaup M, Reinhard P-G, Toepffer C and Zwicknagel G 2003 *J. Phys. A: Math. Gen.* **36** 6165
[30] Jakob B 2007 http://www.opus.ub.uni-erlangen.de/opus/volltexte/2007/469
[31] Jakob B, Reinhard P-G, Toepffer C and Zwicknagel G 2007 *Phys. Rev.* E **76** 036406
[32] Militzer B and Pollock E L 2000 *Phys. Rev.* E **61** 1
[33] See, for example, Landau L D and Lifshitz E M 1959 *Statistical Physics* (London: Pergamon)
[34] Juranek H 2004 *Zustandsgleichung von Wasserstoff bei hohen Drucken im Mbar-Bereich* (Rostock, Dissertation)
[35] Kitamura H and Ichimaru S 1998 *J. Phys. Soc. Japan* **67** 950
[36] Redmer R, Holst B, Juranek H, Nettelmann N and Schwarz V 2006 *J. Phys. A: Math. Gen.* **39** 4479
[37] Ross M 1998 *Phys. Rev.* B **58** 669
[38] Johnson I D The Sesame Data Base (http://www.fas.org/sgp/othergov/doe/lanl/lib-www./la-pubs/00411950.pdf)
[39] Su J T and Goddard W A 2007 *Phys. Rev. Lett.* **99** 185003